JOURNAL OF OPTOELECTRONICS AND ADVANCED MATERIALS Vol. 12, No. 10, October 2010, p. 2052 - 2056

Influence of substrate temperature on structural, optical and electrical properties of evaporated cadmium sulphide thin films

N. M. SHAH, J. R. RAY, M. S. DESAI, C. J. PANCHAL*
Applied Physics Department, Faculty of Technology and Engineering,
The M. S. University of Baroda, Vadodara-390001, Gujarat, India

The hexagonal cadmium sulphide (CdS) thin films with strong (002) orientation is prepared by thermal evaporation technique. The effect of substrate temperature on the structural, morphological, compositional, optical and electrical properties of CdS thin films is investigated. X-ray diffraction and transmission electron microscopy analysis of the films suggests that films presented hexagonal structure and no secondary or mixed phases are found. Scanning electron microscopy images revealed that the grain size increases with T_s while energy dispersive x-ray analysis confirms homogeneity and stoichiometry of films. The analysis of transmission spectra showed that CdS films deposited at different T_s had transmission and energy band gap in the range of 60-90% and 2.32-2.40 eV respectively. Electrical characterization of films deposited at different T_s carried out using Hall effect measurements suggests that films have resistivity and mobility value in the range of 10^4 Ω cm and 2-40 cm^2/Vs respectively influenced by substrate temperature.

(Received March 17, 2010; accepted October 14, 2010)

Keywords: CdS thin film, Substrate temperature, X-ray diffraction, Scanning electron microscopy, Optical and electrical characterization

1. Introduction

In recent years there has been considerable interest in thin film semiconductor because of their use in solar cell devices and thin film transistors for flat panel displays. Cadmium sulfide (CdS) belonging to II-VI group of semiconductors is one of the promising materials studied in the bulk and thin film form as well. Polycrystalline CdS thin films are used in cadmium telluride (CdTe) and copper indium diselenide ($CuInSe_2$) based solar cells, as a window/buffer material for transmitting the light absorbed by CdTe and $CuInSe_2$ [1-2] Thin films of CdS has been prepared by several methods including thermal evaporation [3], sputtering, [4], electrodeposition [5], spray pyrolysis[6], chemical bath deposition [7] etc. Thermal evaporation technique is one of the most effective techniques to deposit CdS thin films due to advantages of reproducibility of films and simplicity. Only recently Solar cells based on $CuInSe_2$ having CdS layer deposited using a dry thermal evaporation technique were reported to obtain efficiencies of 14.5 % almost reaching reference devices using well established CBD deposited technique [8]. For industrial production also an in-line vacuum deposition is preferred over CBD [9]. As it is well known CdS thin films can be grown with α and β phases depending on the deposition conditions. α – CdS invariably grows with columnar structure along the c-axis perpendicular to substrate. This means that there are less grain boundaries parallel to the junction which would impede the flow of photogenerated excess carriers to the grid [10].

In this study we have successfully prepared hexagonal α– CdS thin films useful for solar cell application with excellent preferred orientation of grains along (002) direction by carefully adjusting the source and substrate temperature. The effect of substrate temperature on structural, optical and electrical properties of deposited films has been investigated.

2. Experimental

2.1 Film deposition

CdS thin films of size 1 cm x 1 cm were deposited at different substrate temperatures ranging from 323 K-473 K on glass substrates using CdS powder (99.995%) obtained from Sigma-Aldrich (U.S.A.) by thermal evaporation technique at a base pressure of 10^{-5} m bar. Before deposition substrates were organically cleaned under vapor of methanol, acetone and trichloroethylene. The rate of deposition and thickness of CdS films were 0.1-0.2 nm/s and 50 nm-150 nm respectively, as measured using quartz crystal thickness monitor (Hindhivac (India) DTM -101). The substrate temperature was measured using chromel-alumel thermocouple kept in good thermal contact with the substrate. The thickness of the film for TEM study was 40 nm. This enabled the films transparent to the electron beam.

2.2 Characterization

The structural characterization of CdS thin films deposited at different T_s were carried out using an x-ray

diffractometer (Rigaku D-Max-III) in 2θ range 20º-70º at a scan rate 0.05° s^{-1} with Cu K_α (λ= 0.154 nm) radiation source and transmission electron microscope (TEM) (JEM-2100, JEOL make). The surface and chemical composition analysis of CdS thin films deposited at different T_s were carried out using scanning electron microscope (JEOL, JSM-5610LV) equipped with energy dispersive analysis of x-rays (EDAX) facility. The optical transmittance and reflectance measurements were carried out using the monochromator CM 110, photo detector 816-SL type (Newport) and lock-in amplifier SR-530. For the electrical measurements, four small indium contacts were deposited at room temperature on the surface of CdS films which were arranged symmetrically at four corners. The electrical characterizations of CdS thin films deposited at different T_s were carried out using conventional Hall effect measurements at room temperature under normal light condition using Keithley 614 programmable electrometer and Keithley 181 nanovoltmeter.

3. Results and discussion

3.1 Structural characterization

The crystallographic properties of CdS thin films having thickness of 150 nm deposited at different T_s have been investigated by x-ray diffraction (XRD) technique using Cu K_α radiation source. Fig. 1 shows XRD curves of CdS films deposited at different substrate temperatures.

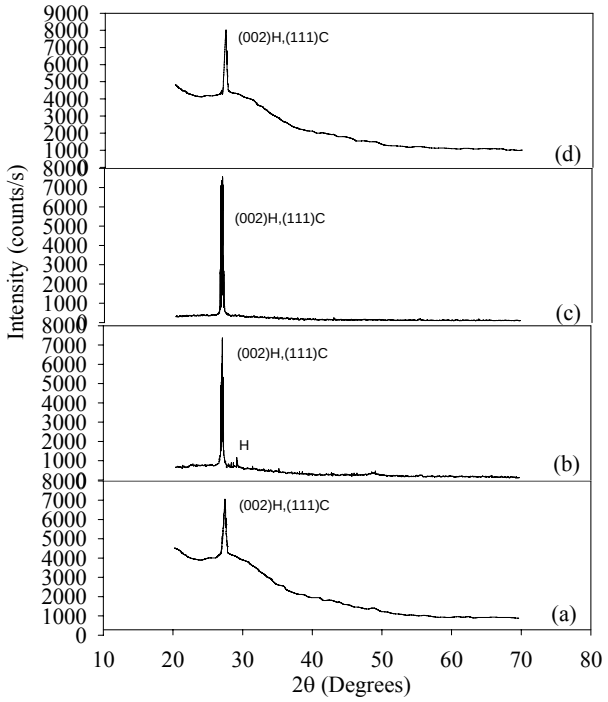

Fig. 1. X-ray diffractograms of the CdS thin films prepared at different substrate temperatures: (a) T_s = 323 K, (b) T_s =373 K, (c) T_s = 423 K, (d) T_s =473 K.

All films showed a predominant single peak at or around 2θ = 27 which can be assigned to the (002) plane of hexagonal or the (111) plane of cubic CdS. This preferred orientation of CdS films is due to the controlled nucleation process associated with the low deposition rate. With increase of T_s, there is an increase in intensity and sharpening of this peak, which is caused by improving crystallinity of films.

XRD analysis of CdS thin films deposited at different T_s revealed that all films had preferred orientation of grains corresponding to (002) diffraction plane of hexagoanal structure or (111) reflections of cubic structure as shown in Fig. 1. Therefore, a straightforward structural characterization of the as-deposited CdS film using XRD is difficult. For solar cell application, hexagonal CdS films are preferable due to its excellent stability [11]. So, to confirm the exact orientation of grains, the structural analysis of film deposited at 373 K is detected with TEM. Sample for TEM study was pealed off from the glass substrate onto copper grid using dilute hydrofluoric acid. Fig. 2 shows TEM with typical selected area diffraction (SAD).

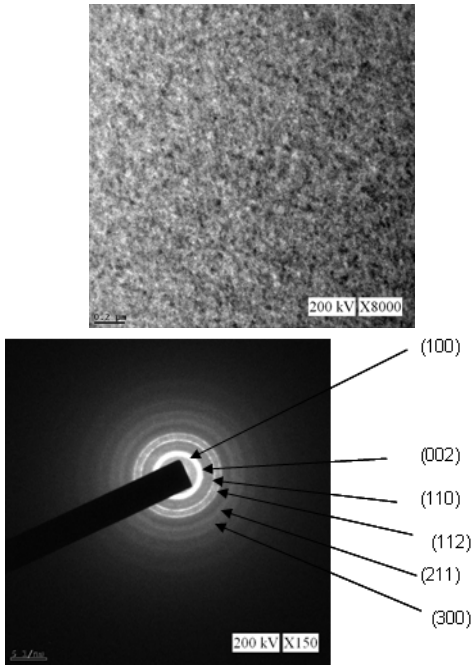

Fig. 2. TEM image and SAD pattern of CdS thin film deposited at 373 K.

The SAD pattern contains sharp rings expected for polycrystalline films. The diameter of rings (D_{hkl}) in the SAD pattern was measured using the formula $d_{hkl} = 2\lambda L/D_{hkl}$. Here, L is the camera length and λ is the wavelength of the electron beam calculated from accelerating potential. The calculated d values corresponds to three characteristic major intensity peaks (002), (110) and (112) matched well with those of the JCPDS data card 41-1049 of hexagonal α- CdS reflections. No cubic phase, complex of cubic and hexagonal or secondary phase is

observed. The very prominent bright ring seen in SAD pattern due to the (002) plane indicates the preferred orientation along that direction. All the obtained (hkl) indices of the diffracted rings matched well with those of the JCPDS 41-1049 data [12] for hexagonal phase.

The mean size of the crystallites in CdS thin films deposited at different substrate temperatures were calculated from the (002) x-ray diffraction peak broadening using the well-known Scherrer's formula [13],

$$d = \frac{0.9\lambda}{B_r \cos\theta} \quad (1)$$

after the correction for the instrumental spectral broadening [14]. Here λ is the wavelength of Cu K_α radiation (λ = 0.154 nm), B_r is the FWHM of (002) peak. The peak position of (002) plane and FWHM of the (002) peak, along with the calculated values of the crystallite size, for films grown at different T_s, are shown in Table 1.

Table 1 The position of (002) peak, FWHM and crystallite size of CdS thin films grown at different T_s

Substrate Temp. (T_s) K	Position of (002) peak (Degrees)	FWHM (Degrees)	Crystallite size (nm)
323	27.31	0.4390	18
373	27.05	0.1732	47
423	27.03	0.1732	50
473	27.14	0.2770	29

3.2 Morphological studies

The as-deposited films were smooth, optically transparent, adherent and green-yellow in color. The surface morphologies of the CdS films deposited at different substrate temperatures is studied using scanning electron microscope (SEM). Fig. 3 shows the SEM images of the surface morphology of the CdS thin films deposited at different T_s.

The SEM images suggest that the microstructures of the CdS films changed depending on the T_s. No pinholes or surface defects were observed in SEM images of CdS films deposited at different T_s. The appearance of cracks in CdS film deposited at 323 K may be due to high tensile stress in the film. A similar observation has also been reported for CdS thin films deposited using CBD [15]. It is worth noting that this surface morphology corresponded to the preferred orientation of (002), as indicated by the XRD patterns in Fig. 1. The increase in the crystallite size would result from the enhancement of the film surface atomic mobility with increasing T_s which enables the thermodynamically favored grains to grow.

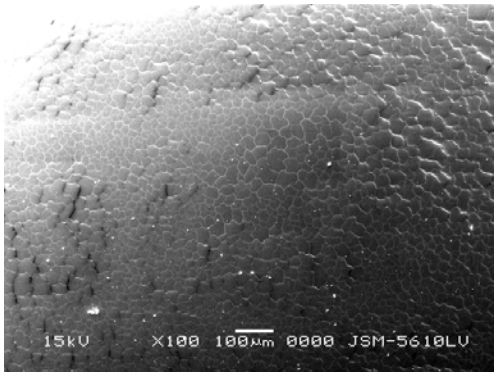

(a)

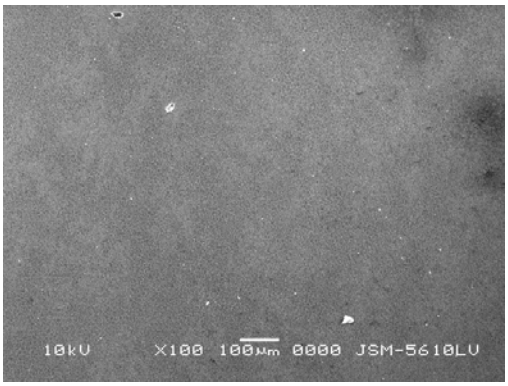

(b)

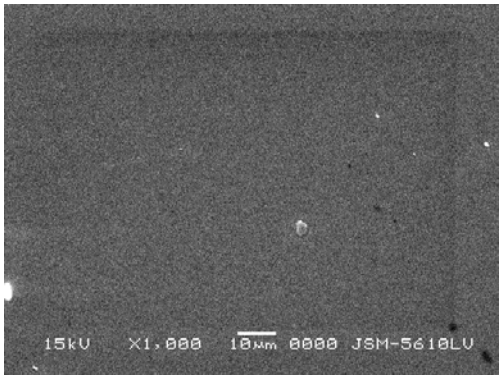

(c)

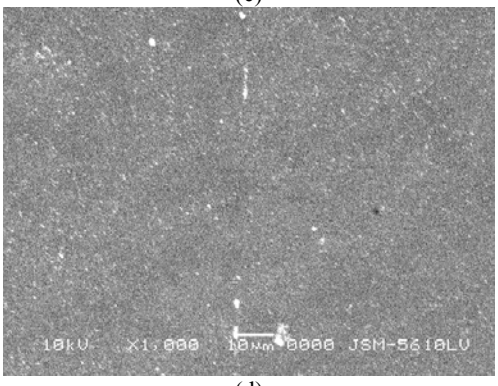

(d)

Fig. 3. SEM micrographs of CdS films deposited at (a) T_s = 323 K, (b) T_s = 373 K, (c) T_s = 423 K, (d) T_s = 473 K.

3.3 Compositional characterization

The energy dispersive analysis of x-rays (EDAX) results shows that the films are more or less stoichiometric. Table 2 shows at. wt. % of CdS thin films of 150 nm deposited at different T_s. The ratio of Cd to S approaches to 1.0 as the substrate temperature approaches to 400 K. However, all the films has some S excess over Cd.

Table 2 EDAX analysis of CdS thin films grown at different T_s

Substrate Temp. (T_s) K	Elemental composition (at.wt. %)		Ratio Cd/S
	Cd	S	
323	49.09	50.91	0.96
373	49.33	50.67	0.97
423	49.93	50.07	0.99
498	49.85	50.15	0.99

3.4 Optical characterization

To a great extent, the application of CdS thin films in optoelectronic devices depends on the optical properties such as transmittance and band gap energy. Fig. 4 shows the transmittance spectra of CdS thin films deposited at different T_s.

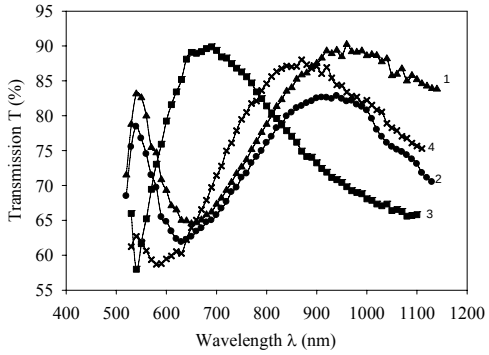

Fig. 4. Transmission spectra of CdS thin films 1) T_s =323 K, 2) T_s =373 K, 3) T_s =423 K 4) T_s =473 K.

It can be seen from the Fig., that the thermally evaporated CdS films were highly transparent in the visible region with about (70-90%) transmission in the visible range. These spectra reveal that films have low absorbance in the visible/near infrared region from 500 nm-1100 nm.

The optical bandgap energy, E_g, (defined as the difference between the top of valence band and the bottom of conduction band) was calculated from the transmittance spectra using the following equation:

$$\alpha = \frac{A}{h\upsilon}\sqrt{h\upsilon - E_g} \qquad (2)$$

where α is the absorption coefficient, A is a constant of proportionality, hν is photon energy and E_g is bandgap energy. Fig. 5 shows plots of $(\alpha h\nu)^2$ with photon energy hν for films grown at different T_s.

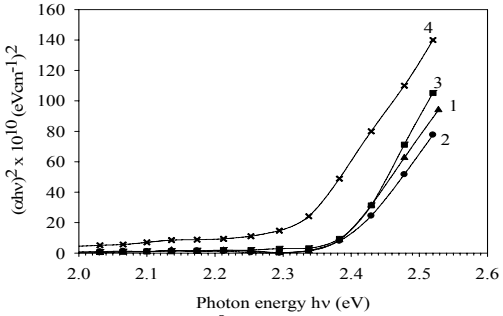

Fig. 5. Plots of $(\alpha h\nu)^2$ vs $(h\nu)$ for CdS thin films 1) T_s =323 K, 2) T_s =373 K, 3) T_s =423 K, 4) T_s =473 K.

Extrapolation of the linear portion of the curve to $(\alpha h\nu)^2 = 0$ gives the band gap energy which is in the range 2.32-2.40 eV which is in good agreement with the band gap values reported in earlier works [16-17]. The band gap value for CdS thin films deposited at different T_s decreases with increase of substrate temperature. The decrease in energy band gap with the substrate temperature is due to the influence of various factors such as crystallite size, structural parameters, deviation from stoichiometry of the film etc. However, we have observed that crystallite size has a direct dependence on T_s. Hence we consider that the observed decrease in energy band gap with increasing T_s is due to increase in crystallite size and decrease in strain and dislocation density.

CdS thin film deposited at 373 K has energy band gap value of 2.40 eV. So, we have further investigated thickness dependence of energy band gap to optimize its thickness for its use as a buffer layer in thin film solar cell based on $CuInSe_2$. Fig. 6 shows that as thickness of the film increases the energy band gap increases. The range of optical band gap is found to lie between 2.33-2.42 eV with increasing film thickness and approaches value of single crystalline CdS (2.42 eV) [18].

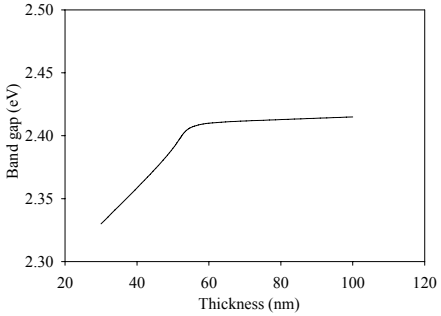

Fig. 6. Dependence of energy band gap of CdS thin films on thickness.

3.5 Electrical characterization

All films deposited during the present investigations have n-type conductivity as verified using hot probe method. The resistivity and mobility value of CdS films deposited at different T_s measured at room temperature under normal light condition is shown in the Fig. 7.

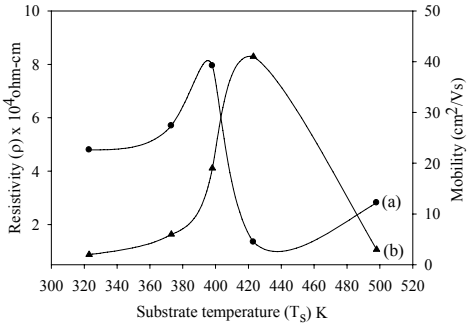

Fig. 7. Variation of (a) Resistivity and (b) mobility of CdS thin films deposited at different T_s.

The resistivity value range from 1.3 x 10^4 Ω cm to 7.9 x 10^4 Ω cm for films with thickness of 150 nm deposited at different T_s. The data show that the resistivity increased as the T_s increased upto 423 K and then decreases with increase of T_s. The high resistivity of CdS films resulted from the good stoichiometry and the lack of defects. The high resistivity of CdS films resulted from the good stoichiometry and the lack of defects. The order of resistivity in the present work is in the range of ~ 10^4 Ω cm, which is suitable for application of CdS films as a buffer layer in thin film solar cells based on $CuInSe_2$. These results of resistivity are quite similar to those obtained by Su and Choy [19] and Ashour et al. [20], on sprayed and vacuum evaporated CdS films by a modified source respectively.The electron mobility value of CdS films increase with T_s, have a maximum at 423 K T_s and decrease thereafter. Similar behavior was observed by Kazamerski et al. [21] for CdS films deposited using thermal evaporation method. The decrease in resistivity with the increase in substrate temperature can be explained using Petritz's barrier model. [22] According to which at low temperatures, the crystallites do not grow sufficiently large while at higher substrate temperature large crystallite sizes are obtained which ultimately decrease the intercrystalline barrier, therefore have to cross comparatively narrow intercrystalline barriers and this result in decrease of resistivity.

4. Conclusions

CdS thin films were deposited on glass substrates held at different temperatures using thermal evaporation technique showed good optical properties and adhered well to the substrates. XRD and TEM pattern of these films indicated that the deposited CdS films contain hexagonal (wurtzite) structure. The crystallite size was found to be 18-50 nm for films deposited at different substrate temperatures. Analysis of SEM images suggests that T_s had obvious affection for the morphology. The increase of T_s improves the surface morphology of the CdS films and also diminishes cracks on the films. The optical and electrical investigations prove that films have high transparency (60-90%), energy band gap in the range of 2.32 eV-2.40 eV and higher value of resistivity.

Acknowledgments

N M Shah is grateful to UGC (WRO Pune, India) for the award of teacher fellowship under "Faculty Improvement Program" in X^{th} plan. Authors also wish to thank UGC (New Delhi, India) for providing financial assistance through major research project.

References

[1] P. Ketrush, P. Gashin, V. Nikorich, V. Suman, J. Optoelectron. Adv. Mater. **7**(2)**,** 795 (2005).
[2] I. Salaoru, P. A. Buffat, D. Laub, A. Amariei, N. Apetroaei, M. Rusu, J. Optoelectron. Adv. Mater. **8**(3), 936, (2006).
[3] D. S. Reddy, B. Kang, Seong-Cho Yu, K. R. Gunasekhar, K. N. Rao, A Divya, P. S. Reddy, J. Optoelectron. Adv. Mater. **9(12),** 3747, (2007).
[4] F. El Akkad, M. Abdel Naby, Solar Energy Materials **18**, 151, (1989).
[5] R. K. Sharma, Kiran Jain, A. C. Rastogi, Current Applied Physics **3**, 199, (2003).
[6] G. Sasikala, R. Dhnasekaran, C. Sbramanian, Thin Solid Films **30**, 71, (1997).
[7] H. Metin, F. Sat, S. Erat, M. Ari, J. Optoelectron. Adv. Mater. **10**(10), 2622, (2008).
[8] M. Rusu, Th. Glatzel, A. Neissser, C. A. Kaufmann, S. Sadewasser, M. Ch. Lux-Steiner, Appl. Phys. Lett. **88**, 143510, (2006).
[9] D. Abou-Ras, G. Kostorz, A. Romeo, D. Rudmann, A. N. Tiwari, Thin Solid Films **480-481**, 118, (2005).
[10] G. Sasikala, P. Thillakan, C. Subramanian, Solar Energy Materials and Solar cells **62**, 275, (2000).
[11] C. Y. Yeh, Z.W. Lu, S. Froyen, A. Zunger, Phys. Rev. B **46**, 10086, (1992).
[12] Powder Diffraction File, Joint Committee on Powder Diffraction Standards, ASTM (1998) (Card no. 41-1049).
[13] C. S. Barett, Structure of Metals, Crystallographic methods, Principles and Data, McGraw-Hill, New York, (1956) p.156.
[14] U. Pal, S. Saha, B. K. Samantaray, H. D. Banerjee, A. K. Chaudhuri, Phys. Status Solidi A **111**, 515, (1989).
[15] A. Mandoza-Galvan, G. Martinez, R. Cozda-Morales, J. Appl. Phys. **80**, 3333, (1996).
[16] C. T. Tsai, D. S. Ohuu, G. L. Chen, S. L. Yang, J. Appl. Phys. **79**, 9105, (1996).
[17] N. Lovergine, R. Cingolani, A. M. Mansini, J. Crys. Growth, **118**, 304, (1992).
[18] S. M. Sze, Physics of Semiconductor Devices, Wiley Eastern Limited, New Delhi, 1986.
[19] B. Su, K. L. Choy, Thin Solid Films **359**, 160, (2000).
[20] A. Ashour, N. El-Kadry, S. A. Mahmoud, Thin Solid Films **269**, 117, (1995).
[21] L. L. Kazmerski, W. S. Berry, C. W. Allen, J. Appl. Phys. **43**(8), 3515, (1972).
[22] R. L. Petritz Physical review **104**(6), 1508, (1956).

*Corresponding author: cjpanchal_msu@yahoo.com